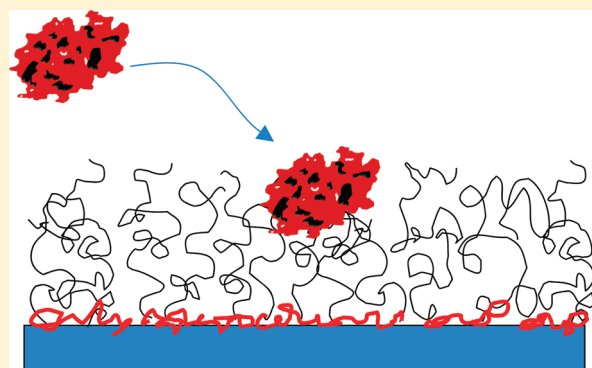


Interaction of Cationic Proteins and Polypeptides with Biocompatible Cationically-Anchored PEG Brushes

S. Gon,[†] B. Fang,[‡] and M. M. Santore^{‡,*}[†]Department of Chemical Engineering and [‡]Department of Polymer Science and Engineering, University of Massachusetts, Amherst, Massachusetts 01003, United States

Supporting Information

ABSTRACT: Poly(ethylene glycol) (PEG) brushes, for instance, physically tethered to a surface via the adsorbing portion of a PEG-containing copolymer, are a popular protein-resistant surface treatment. Though physisorbed brushes might be displaced by competing species, they continue to dominate diagnostic chips and other applications. In this work, we examine the interactions of two cationic species, poly L-lysine (PLL) and lysozyme, with a popular type of PEG brush, formed by the adsorption of a graft copolymer of PLL–PEG on negative silica. Here, 20K molecular weight (MW) PLL comprises the main backbone that adsorbs to the silica and the PEG side chains (2K or 5K, in different samples) form tethers. This work examines variations in brush heights and densities, still confining the study to brush architectures (near 30% functionalization of the PLL by PEG side chains) that completely prevent the adsorption of blood proteins such as fibrinogen and albumin. It is found that lysozyme adsorbs to interfaces passivated with these PLL–PEG copolymers in amounts that increase with the amount of PEG in the brush. This suggests attractions between the PEG tethers and lysozyme itself. When PLL–PEG brushes are challenged by homopolymer PLL (a random coil at the physiological pH studied here), the PLL–PEG is almost completely displaced from the silica substrate. The rapid displacement kinetics (with complete loss of protein repellence) for all brush architectures suggest the absence of a steric barrier against PLL penetration of the PEG brush. A small overshoot in surface coverage prior to the displacement of the PLL–PEG chains demonstrates the adsorption of PLL on regions of silica at the base of the brush prior to chain displacement, further arguing for the accessibility of the substrate despite the presence of the brush. Differences between the interactions of lysozyme or PLL with the brush suggest an important role of the globular nature of folded proteins compared with random coil polypeptides in protein–brush interactions and brush penetration. The results emphasize the technological challenge of retaining seemingly robust brushes adsorbed to interfaces, and eliminating protein adhesion from the brush itself.



INTRODUCTION

Despite advances that enable growth of covalently attached brushes from surface-bound initiators, economic considerations drive continued interest in brush formation from the adsorption of PEG (poly(ethylene glycol))-containing copolymers. For hydrophobic surfaces, amphiphilic copolymers are an obvious choice to create PEG-tethered surfaces from aqueous formulations; however, complications can arise from micelles in solution and on surfaces. For negative surfaces, copolymers of PEG and polycations are a useful route to produce surfaces with PEG tethers. Here, the adsorbing polycation is self-repellant and avoids the aggregation and micellization-based complications that occur with polymer amphiphiles. Indeed, several laboratories have developed libraries of PEG–PLL (PEG–Poly L-lysine)^{1–4} and PEG–PEI (PEG–poly(ethylene imine))^{5,6} copolymers, containing at least some members that are exceptionally protein resistant, adsorbing 0.01 mg/m² or less from serum. Also, Messersmith has pioneered the creation of DOPA (3,4-dihydroxyphenylalanine)-containing PEG, most appropriate as

a protein-resistant coating for TiO₂ implants.⁷ A close comparison between the best PLL–PEG copolymers and the PEG–DOPA polymers reveals a slight superiority of the former's protein resistance *in vitro*,⁸ while the significance of this difference for *in vivo* applications is unclear. Indeed, current indicators suggest that in the long run, the DOPA-based anchors, though appropriate for only limited substrate chemistries, are the better choice *in vivo*.⁷

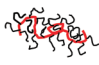
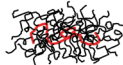

Beyond the chemical instability of PEG, a problem for any physisorbed copolymer-based brush is its potential for displacement by competing species. While biomedical studies have not revealed exactly which proteins may be responsible, arguments from polymer physics suggest that cationic proteins, polymers, and polypeptides can destabilize PEG brushes anchored by cationic chains on negative substrates. High molecular weight

Received: June 29, 2011

Revised: August 24, 2011

Published: September 16, 2011

Table 1. Copolymer Samples and Schematics

	Polymer I	Polymer II	Polymer III
			
	PLL-(2.7)PEG(2K)	PLL-(2.2)PEG(5K)	PLL-(4.7)PEG(5K)
PEG MW	2,000	5,000	5,000
Grafting Ratio	2.7	2.24	4.5
% PLL Functionalization	37%	45%	22%
Molecular Weight	136,000	367,000	188,000

PLL-20K
(157 repeats)



homopolymers will displace, ultimately, low molecular weight chains of identical chemistry,^{9,10} while densely charged polyelectrolytes will displace chains of lower charge density but similar length.¹¹

These rules of thumb apply to the anchoring constituent of PEG-polycation adsorbed brushes. Thus, efficient cationic challengers for brush displacement could include the PLL-homopolymer itself, since functionalization of PLL with PEG chains reduces the cationic functionality of the backbone, and since the PLL anchor of the copolymer must also pay the entropic “cost” of stretching its PEG tethers.¹² The question, then, is to what extent can cationic challengers, such as positively charged proteins or PLL itself, penetrate the PEG corona and displace the PLL anchors. Since brushes with about $\sim 1 \text{ mg/m}^2$ of PEG tethers have been documented to be protein-resistant,^{2,8,13} it is interesting to ask whether this resistance translates to an impermeability toward challenging species, at least ones that are peptide-based. Indeed, if a brush is thick enough to shield the underlying substrate from approaching proteins, then it may be stable against exchange for very long periods, despite a driving force favoring exchange.

This paper examines brushes formed from PLL–PEG copolymers physisorbed on silica. Following the literature from the Hubbell, Voros, and Textor groups, this study focuses on architectures which have been previously established to be highly protein resistant, adsorbing less than 0.01 mg/m^2 of serum protein at physiological pH and ionic strength.^{8,13} These brushes are thicker (8–16 nm) than the range of electrostatic interactions. We reproduce the stability of these surfaces against adsorption of albumin, fibrinogen, and other negative proteins, but observe that cationic protein adsorption occurs and that brushes can be destroyed by exposure to cationic polypeptides. The observations prompt reconsideration of the general assumption of protein–PEG repulsions and the ability of polypeptides to penetrate relatively thick PEG brushes.

EXPERIMENTAL PROCEDURES

PLL–PEG copolymers were synthesized as described previously:^{14–16} Poly-L-lysine hydrobromide (PLL) with a nominal molecular weight of 20 000 from Sigma-Aldrich was dissolved in 50 mM pH 9.1 sodium borate buffer. Two different PEG molecular weights were employed, either 2000 or 5000. For copolymers containing 2K PEG, the *N*-hydroxysuccinimidyl ester of methoxypoly(ethylene glycol) acetic acid (Layson Bio Inc.) was added, and the solution was stirred for 6 h. For copolymers containing 5K PEG, this reactive compound was not

available and PEG sodium valeric acid (PEG–SVA) was employed instead. After reaction, the mixture was dialyzed against pH 7.4 phosphate-buffered saline for 24 h, dialyzed against DI water for another 24 h, and then freeze-dried and stored at -20°C . The relative amounts of PEG and PLL were varied, with the grafting ratio defined to be the number of PLL monomers per PEG side chain. This is inversely proportional to the percent functionalization of the PLL by PEG.

Purified copolymers were characterized in D_2O using ^1H NMR on a Bruker 400 MHz instrument. The grafting ratio was determined from the relative areas of the lysine side-chain peak ($-\text{CH}_2-\text{N}-$) at 2.909 ppm and the PEG peak ($-\text{CH}_2-\text{CH}_2-$) at 3.615 ppm. Table 1 summarizes the molecular properties of the three samples employed in this study. While other molecular architectures were synthesized, these particular three samples were studied further because the brushes they formed on adsorption to silica eliminated the adsorption of key serum proteins, consistent with prior literature.¹³

Polymer brushes were formed by adsorbing copolymers from flowing phosphate buffered solution (0.008 M Na_2HPO_4 and 0.002 M KH_2PO_4 , pH 7.4, with Debye length $\kappa^{-1} = 2 \text{ nm}$, 100 ppm copolymer) over acid-etched microscope slides (these surfaces are silica) in slit shear laminar flow cells at gentle flow conditions (wall shear rate $= 5.0 \text{ s}^{-1}$) for 20 min. This was followed by continued flow of the same buffer for another 20 min. Optical reflectometry,¹⁷ run *in situ*, was used to track the adsorption process and determine the ultimate mass of adsorbed copolymer. When needed, total internal reflectance fluorescence (TIRF) was employed to track the adsorption or desorption of a fluorescently tagged species during competitive challenge experiments. This instrument was described previously¹⁸ and, notably, employs the same flow chamber as the reflectometer.

The polymers and proteins used to challenge the adsorbed PLL–PEG brushes were purchased from Sigma-Aldrich and used as-is. These included hen egg white lysozyme (L6876), bovine serum albumin A (7511–10G), bovine fibrinogen (F8630–1G, fraction 1, type 1S), equine skeletal muscle myoglobin (M0630–1G), and alkaline phosphatase (P7640–1G). Notably, the PLL homopolymer used to challenge the brush was the same PLL employed as the anchoring group of the copolymer. In cases where TIRF was employed to track PLL adsorption, it was made fluorescent by labeling with fluorescein-isothiocyanate (FITC isomer I, F250–2 from Aldrich). Labeling and purification were conducted as previously described.¹⁹ Challenge experiments were conducted in the same flow chamber used to deposit brushes, with continuous flow of the various solutions and buffers, and the same flow rate. Studies at Debye lengths other than 2 nm were done either in dilute (overall concentration of 0.005 M for $\kappa^{-1} = 4 \text{ nm}$) or concentrated buffer for $\kappa^{-1} = 1 \text{ nm}$.

In some studies, small amounts of PLL were adsorbed to bare silica surfaces prior to the adsorption of the PLL–PEG brush. This was

carried out as a sequence of carefully timed adsorption steps in a single flow chamber. Control of the particular small PLL amount was achieved through the use of dilute PLL solution (5 ppm) and careful timing of PLL flow and reinjection of buffer, so that controlled deposition, not full surface saturation, occurred. Subsequent adsorption of the brush was carried out by flowing PLL–PEG solution for a time appropriate to saturate the surface. Buffer was reinjected only after a clear plateau was demonstrated. This procedure has been documented in detail previously.¹⁶ It was additionally shown that (1) initial PLL adsorption did not produce surface aggregates and that PLL chains were well-distributed about the surface; and (2) initially adsorbed PLL was not displaced by subsequently adsorbing PLL–PEG.¹⁶

ζ potential measurements, intended to gauge the electrostatic features of planar brush-bearing surfaces, were conducted using 50 ppm suspensions of 1- μ m silica spheres (from GelTech, Orlando) as a model for the planar silica surfaces. Polymers were adsorbed to the particles to create PLL- or brush-covered silica, using an amount of polymer appropriate to saturate the surface and known the specific area of the microparticles. Particles were incubated overnight prior to measurement of their ζ potential in a Malvern Zeta Sizer Nano ZS instrument.

RESULTS

Characterization of Brushes. Optical reflectometry measurements of the adsorbed amounts of each of the three copolymers are summarized in Table 2. From this, along with knowledge of the molecular architecture and PEG content of the copolymers, it was possible to deduce the structure of the three brushes, according to the Alexander–DeGennes model,^{20,21} in Table 2. The PEG and PLL copolymer content from NMR in Table 1 enabled a calculation of the PEG and PLL content in each adsorbed brush (from a measurement of the total interfacial mass). Then from the PEG content of each brush, and the known molecular weight of the PEG tethers (2000 or 5000) in each brush, the number of PEG tethers per unit area followed. Inversion of this quantity enabled a calculation of the area per tether. The blob diameter (or tether spacing, also equal to the brushes' persistence length) is the square root of this tether area.

An important point in Table 2, the PLL content of all three brushes (presumably at the brush base) is substantially less than a saturated PLL layer of the same molecular weight, while the graft spacing of the PEG tethers is smaller than the calculated free coil diameter (the root-mean-square end-end distance): 4.7 nm for 2K PEG, and 8.2 nm for 5K PEG. This suggests that the PEG tethers are stretched normal to the surface, as required in brushes.

The calculation of the brush height follows from the average spacing between tethers, giving the brush's persistence length. An assumption of $N^{3/5}$ (good solvent) scaling of the chain inside each blob (at distances less than a persistence length) allows calculation of the number of blobs in the brush, as previously described, using reported values of 0.57 nm for the length of a Kuhn step and 59 g/mol for the molecular weight of a Kuhn segment.^{16,22} That is, the number of blobs in a brush is the total number of Kuhn steps in a tether, divided by the number of Kuhn steps in a blob. For instance for Brush #1, $N_{\text{tether}} = 2000/59 = 34$ and $N_{\text{blob}} = (1.9 \text{ nm}/0.57 \text{ nm})^{5/3} = 7.4$. This gives $34/7.4$ blobs in Brush #1. The brush height follows as the product of the number of blobs times the blob diameter, $4.7 \times 1.9 \text{ nm} = 9 \text{ nm}$ for Brush #1.

Notably, Brush #1 is shorter than the others but still substantially thicker than the 2 nm Debye length in the main study, while

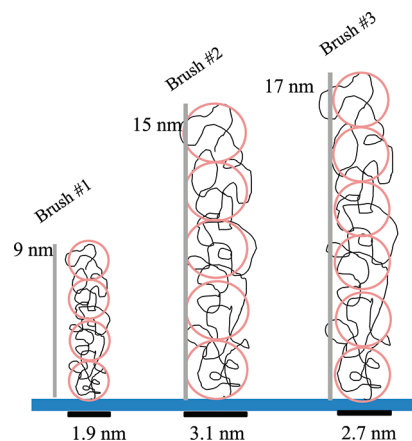


Figure 1. Structure of the PEG tethers within the three brushes, calculated according to the Alexander–deGennes treatment, showing graft spacing or brush persistence length, equal to the “blob” size. Also shown is the number of blobs in each brush.

the two thicker brushes are nearly similar in height but differ in their PEG/PLL content and in the effective number of “blobs” per tether. These estimates are conceptualized in Figure 1.

While the literature suggests that electrostatic effects should be unimportant at the 2 nm Debye length of this study, an assessment of the electrokinetic surface character is useful. The lower part of Table 2 reveals, via ζ potential, a net negative interface for all brushes. That the surfaces have an underlying negative charge is not surprising: The silica substrate is substantially negative and a PLL layer adsorbed to saturation (0.4 mg/m²) only slightly overcompensates the underlying surface charge. The surfaces, with their PLL content less than that of a fully saturated PLL layer, will therefore be negatively charged in region where the PEG is anchored. That the negative interfacial potential can be sensed hydrodynamically via ζ potential suggests that the shear plane penetrates the brush somewhat. The ζ potential is still substantially reduced (in magnitude) for these brush-containing surfaces compared with surfaces with similar PLL loading but no PEG. The extent to which proteins can sense the negative interfacial environment (do they penetrate the brush more or less than the shear plane?) is addressed below.

Interactions with Globular Proteins. Table 3 summarizes the adsorption of several proteins on the three brushes at a Debye length of 2 nm. In general, proteins with a net negative charge, regardless of size or shape, do not adsorb to the brushy surfaces, while cationic proteins and polypeptides do adhere. In the case of lysozyme with a net charge of 7+ to 8+, substantial adsorption is observed for the thicker brushes, with the greatest adsorption on Brush #2, which contains the greatest mass of PEG. Notably, the efficient elimination of negative protein adsorption (albumin, fibrinogen, and others) on these brushy surfaces reproduces reports in the literature for a lack of adsorption from serum.^{13–15} Indeed the lack of serum adsorption was the basis our choice of these brush architectures (and in particular the grafting ratio).

The adsorption traces for lysozyme on the three brushes are detailed in Figure 2, and run contrary to current thinking about protein-brush interactions. First, it is generally accepted that protein repellence occurs when brushes are sufficiently thick to screen electrostatic and van der Waals attractions. Second, studies comparing the adsorption of lysozyme and fibrinogen over a series of PEG-containing or zwitterionic surfaces typically

Table 2. Brush Architecture and ζ Potentials

	PLL	Brush #1	Brush #2	Brush #3
	homopoly 20K	PLL-(2.7) PEG(2K)	PLL-(2.2) PEG(5K)	PLL-(4.7) PEG(5K)
saturated adsorption, mg/m ²	0.4	1.1	0.9	1.3
adsorbed PEG, mg/m ²	0	0.94	0.85	1.16
adsorbed PLL, mg/m ²	0.4	0.16	0.05	0.14
area/copolymer, nm ²	83	206	680	247
area/PEG tether, nm ²		3.6	9.6	7.2
"blob" diameter, or tether spacing, nm		1.9	3.1	2.7
number of blobs		4.7	5.1	6.4
brush height, nm		9	15.5	17.2
ζ (1 nm), mV [$\zeta_{\text{SiO}_2} = -57$ mV] etc	2 ± 5	-4 ± 3	-11 ± 3	-4 ± 3
ζ (2 nm), mV [$\zeta_{\text{SiO}_2} = -73$ mV] etc	6 ± 3	-9 ± 3	-19 ± 3	-10 ± 3
ζ (4 nm), mV [$\zeta_{\text{SiO}_2} = -84$ mV] etc	4 ± 3	-21 ± 3	-34 ± 3	-25 ± 3

Table 3. Protein Adsorption at $\kappa^{-1} = 2$ nm, pH 7.4^a

	MW	dimensions, nm \times nm \times nm	charge, pI	protein adsorption, mg/m ²		
				Brush #1	Brush#2	Brush#3
fibrinogen, bovine serum	340 000	4.5 \times 4.5 \times 47	-8 to -10, ²³ 5.8 ²⁴	0–0.02	0	0
albumin, bovine serum	68 000	4 \times 4 \times 14	-9, 4.8 ²⁵ –5.1	0	0	0
myoglobin	17 000	4.4 \times 4.4 \times 2.5	-, 6.8–7.0 ²⁶	0–0.02	—	—
alkaline phosphatase, monomer (bovine)	81 000	9 \times 4 \times 4	-, 5.7 ²⁷	0	—	—
lysozyme, hen egg white	14 300	3 \times 3 \times 5	+7 - +8, 11 ^{26,28}	0.05R	1.0R	0.2R
poly(L-lysine)	20 000	random coil	+++	0.4E	0.4E	0.4E

^a Key: R = substantially reversible adsorption. E = Exchange (displacement) of previously adsorbed brush.

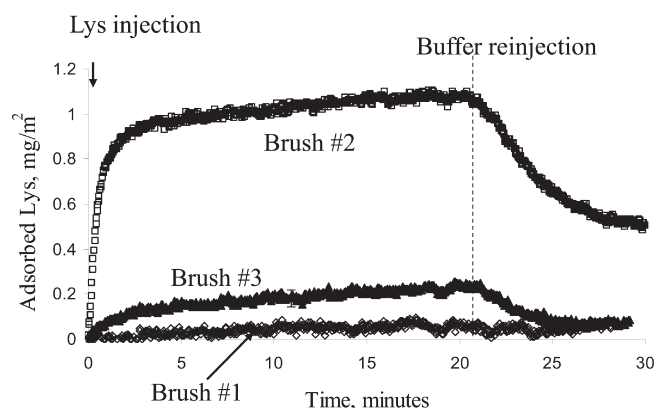


Figure 2. Lysozyme adsorption onto three brushes at pH 7.4 and $\kappa^{-1} = 2$ nm, followed by rinsing, near 20 min.

show parallel reduction in the adsorption of both proteins.^{29,30} These studies often have focused outside the materials design space where surfaces, such as Brush #2 of the current study, are overloaded with PEG and are stable against serum proteins but adhere lysozyme. Indeed a comprehensive study employing libraries of PLL–PEG and DOPA–PEG polymers suggests that the most important feature of a brush is the tethered PEG mass: If it is about 1 mg/m² or greater, good resistance to serum proteins is observed, independent of PEG chain length or grafting density (for PEG lengths in the range from 1K to 5K).⁸ Figure 2 shows the opposite. The thinnest brush, #1, adsorbs practically no lysozyme, while the thicker brushes adhere more

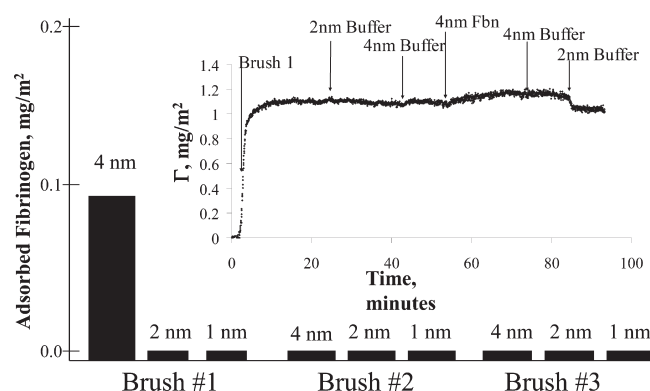


Figure 3. Fibrinogen adsorption on brushes for different ionic strengths. Note reversible adsorption on Brush #1 when the ionic strength is switched (inset) from the mildly adsorbing conditions at $\kappa^{-1} = 4$ nm down to 2 nm.

lysozyme. This suggests, first, that the attractions between lysozyme and the interface are between the protein and the PEG, not between the protein and the underlying substrate. (Notably lysozyme–substrate interactions are electrostatically attractive, but apparently well-screened by the thinnest of the brushes, #1.) Instead, the increasing protein retention with PEG content suggests specific interactions between PEG and lysozyme, not available to the other proteins.

The claim that lysozyme adsorption does not result from electrostatic attractions to the underlying silica must be substantiated by a similar lack of interaction between the anionic

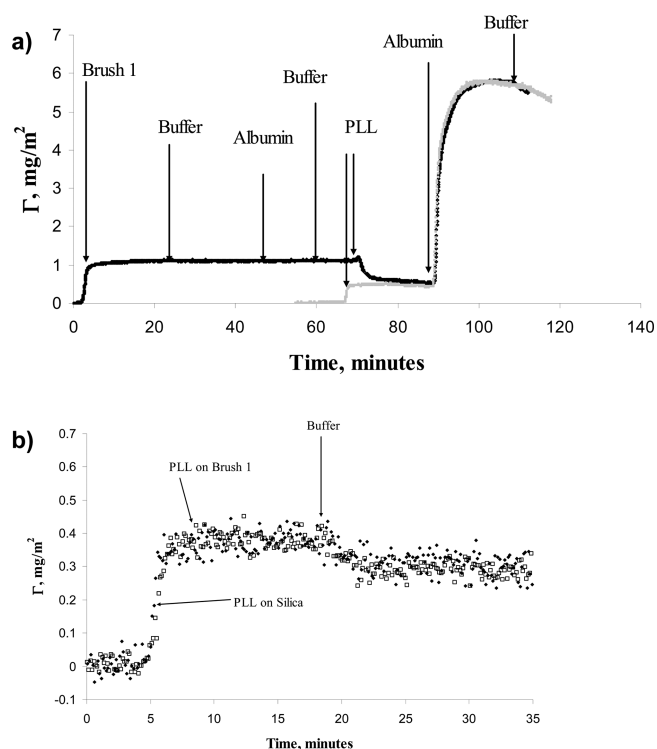


Figure 4. (A) Adsorption and PLL challenge of Brush #1 in buffer with $\kappa^{-1} = 2$ nm. The original brush is exposed to 100 ppm albumin before and after the PLL challenge, using 100 ppm PLL solution. (B) Adsorption of fluorescently labeled PLL, measured by TIRF onto a bare silica surface (solid symbols), and during the challenge of Brush #1 (hollow symbols). In the latter, the behavior of PLL–PEG chains are not seen since they are not fluorescently tagged.

protein and the brush-covered silica. Figure 3 considers the influence of Debye length on the adsorption of fibrinogen, chosen as a model negative protein because it is well studied and known to adsorb onto positive³¹ and negative surfaces (including silica at pH 7.4).^{32–34} On negative surfaces, electrostatic attractions involve fibrinogen's cationic groups, evidenced by the impact of ionic strength.^{32,33} Figure 3 demonstrates that for $\kappa^{-1} = 4$ nm, fibrinogen adsorbs onto Brush #1 but not Brush #2 or #3. This suggests an attraction between fibrinogen and the underlying substrate, screened by the thicker brushes. That this attraction is electrostatic in origin is further supported, in Figure 3, by the observed lack of fibrinogen adsorption to all three brushes at κ^{-1} of 1 and 2 nm, conditions where the steric brush repulsions screen electrostatic interactions. The argument is further strengthened by the reversibility of the fibrinogen adsorption on Brush #1 with changing ionic strength. Long range electrostatic attractions at 4 nm may draw fibrinogen to the brush periphery, but without stronger interactions the silica or train layer, fibrinogen is immediately and completely released when the ionic strength is raised. The fast rate of protein release suggests fibrinogen adsorption (at 4 nm) on top of the brush.

Thus, we deduce that at 2 nm, the conditions for most of this study, the brushes fully screen electrostatic interactions between the proteins and silica. Therefore, the net-negative character of the nonadsorbing proteins in Table 3 is not directly (through electrostatic repulsions) responsible for their lack of adsorption.

Interactions with PLL. Table 3 notes that PLL solutions displace PLL–PEG from the silica. An example of PLL challenge of Brush #1 is shown in Figure 4A, a reflectometry trace including

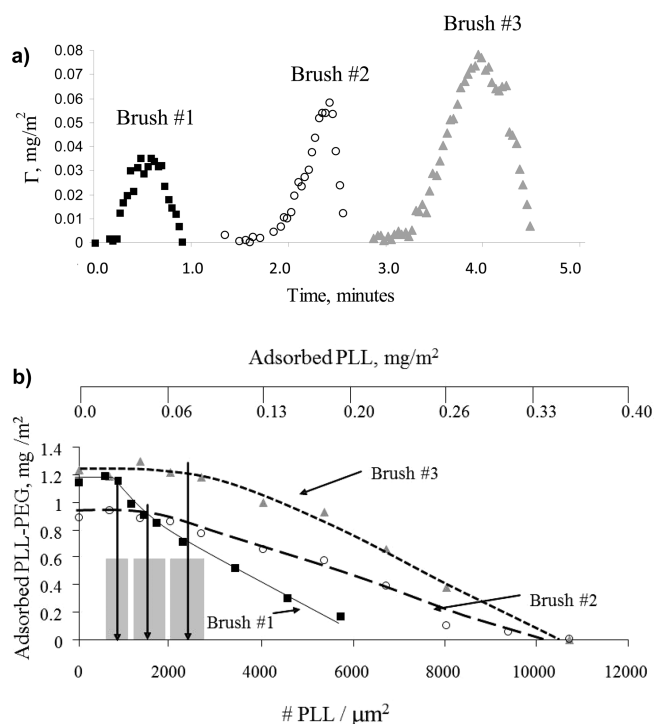


Figure 5. (A) Close up of overshoot portion of reflectometry runs in which PLL challenges preadsorbed PLL–PEG brushes. The time axis for the different runs is shifted to facilitate a comparison of the overshoot seen for the different brushes. (B) Amount of PLL–PEG backfill adsorbing to silica after the initial adsorption of small amounts of PLL, on the x-axis. Gray bars indicate uncertainty in determining the x-axis values where the data start to turn down. Lines are drawn to guide the eye.

multiple steps: initial adsorption of PLL–(2.7) PEG–2K to form Brush #1; its retention on the surface during rinsing in pH 7.4 $\kappa^{-1} = 2$ nm buffer; challenge by albumin solution (in the same buffer, nothing happens); and subsequent challenge by PLL solution (100 ppm). Brush exposure to PLL causes the surface coverage to decrease from 1.1 mg/m² to 0.4 mg/m². The latter is characteristic of a saturated PLL layer on silica, and indeed, when albumin is exposed again to the surface, it adsorbs rapidly. The gray data set on the same graph shows the adsorption of PLL on a bare silica surface and subsequent albumin adsorption. The latter is kinetically identical to albumin adsorption on a surface initially containing a PLL–PEG brush (#1), after PLL challenge. This suggests that the brush is completely displaced by PLL as though the brush were never present. The technical implications of the subsequent protein adsorption are clear.

The rapid kinetics of the PLL/PLL–PEG exchange process are striking. The loss of PLL–PEG from the silica is clear in Figure 4A, but adsorption of PLL into the brush is equally fast, in Figure 4B. Figure 4B demonstrates identical kinetics for PLL adsorption on bare silica and PLL adsorption (measured via TIRF with FITC-tagged PLL) into Brush #1. Brush #1 presents no kinetic barrier to the penetration of PLL, and apparently the segmental exchange at the base of the brush is rapid. Fast PLL adsorption kinetics (in the Supporting Information) occur for PLL challenge Brushes #2 and #3, only slightly slower than observed for Brush #1, with 0.4 mg/m² of PLL established in under 2 min. Likewise, in the Supporting Information, the evolution of the interfacial mass upon PLL challenge of Brushes #2 and #3 is similar to Brush #1 in all but quantitative details.

Figure 4A documents a small but interesting overshoot (near 70 min) in the total interfacial mass during PLL challenge of PLL–PEG brushes. This feature is seen, in Figure 5A, for all 3 brushes, though it varies quantitatively. The overshoot suggests that a small amount, 0.03–0.08 mg/m², of PLL adsorbs on the silica before the PLL–PEG starts to be displaced. The possibility of this incremental adsorption is reinforced by Table 2: The amount of PLL anchored at the base of these brushes, 0.05–0.16 mg/m², is considerably less than the PLL saturation coverage on a bare silica surface, 0.4 mg/m². Also interesting, in Figure 4B, PLL adsorbs continuously during the overshoot and subsequent PLL–PEG displacement processes, near the transport-limited PLL adsorption rate.

Figure 5B argues, based on a different type of experiment, that some PLL can be accommodated at the base of an adsorbed PLL–PEG brush. Here, small amounts of PLL were adsorbed to a bare silica surface, followed by adsorption of a saturated PLL–PEG brush on the remaining surface. Figure 5B summarizes the amount of PLL–PEG accommodated after PLL preadsorption: Small amounts of PLL do not affect the PLL–PEG coverage, and are tolerated at the base of the brush. However, there is a maximum amount (depending on the particular PLL–PEG sample) of PLL that can be accommodated before PLL–PEG adsorption is reduced, indicated by the vertical bars, whose width indicates the level of uncertainty. Notably, for the three different PLL–PEG architectures, the amount of preadsorbed PLL that can be accommodated without compromise of a subsequently adsorbed brush is similar to that which can be adsorbed into an existing brush before the PLL–PEG is displaced. The latter is given by the overshoots in Figure 5A.

DISCUSSION

Adhesion to Interfaces, Penetration of the PEG Corona, and Exchange of Trains. Of the proteins studied, those with negative charge did not adhere to brushy surfaces, while those with net positive charge were attracted to the brushes or to the underlying negative substrates. The observed correlation between adsorption and the sign of the protein charge implicates electrostatic protein–surface interactions, with the negative proteins being repelled from the underlying negative substrates. The increased fibrinogen adhesion at lowered ionic strengths (Figure 3) only on the thinnest Brush #1, however, clarifies that electrostatic repulsions from the silica could not be responsible for the nonadherence of the negative proteins at $\kappa^{-1} = 2$ nm. Indeed Figure 3 parallels findings from the literature with serum proteins, for the effects of brush thickness and ionic strength.¹ It was necessary to reproduce this trend with our own materials to ensure the conformance of our brushes to the literature. The importance of this result lies (1) in its reaffirmation (for our materials) of the substantially greater brush thicknesses compared with the 2 nm Debye length (eliminating electrostatic protein–substrate interactions) and (2) in the contrasting behaviors of negative proteins and of lysozyme and PLL. Thus, the surprising influence of the net protein charge on protein interactions with brushy surfaces cannot be attributed to electrostatic protein–substrate (silica or train layer) interactions.

It is interesting to note the negative ζ potentials of the brushy surfaces, significant for two reasons: First, it may seem counterintuitive that Brush #1 had more mildly negative ζ potentials than thicker Brushes #2 or #3. All other things constant, the magnitude of the ζ potentials should decrease with increasing brush

thickness because the thicker brushes push the shear plane further out from the surface.¹² Table 2 reveals, however, differing amounts of PLL at the base of these brushes, altering the effective surface potential in the train layer of the brush. For instance, while Brush #1 is thinner than Brush #2, Brush #1 also contains more PLL at its base. Therefore, the surface potential beneath Brush #1 will be less negative than Brush #2. A second important point is that while the ζ potentials reveal the electrostatic environment at some point inside the PEG brush (due to some penetration of the shear plane into the brush), globular proteins seem not to access this electrostatic environment at $\kappa^{-1} = 1$ or 2 nm. That is, the shear plane during a ζ potential measurement penetrates the brush more than globular proteins.

An observation which was not previously documented, to our knowledge, is the adhesion of lysozyme to relatively thick PEG brushes. (While Pasche has studied lysozyme interactions with PLL–PEG on Nb₂O₅ surfaces, those copolymers contained 2K PEG tethers and all but one system were thin brushes that did not completely screen the electrostatic potential from the underlying substrate.¹ Indeed, current results with PLL(2.7)-PEG-2K (similar to one protein-resistant specimen within the Pasche study) produce very slight lysozyme adsorption in agreement with that their findings.) Figure 2 argues in favor of PEG–lysozyme attractions, a possibility which runs contrary to mainstream thinking that PEG ubiquitously repels globular proteins through steric (osmotic) interactions, as a result of the (1) the lack of charge on PEG, (2) its tendency to be well-solvated in water, with a net repulsion toward other molecules that are also water-solvated and (3) its hydrogen-bond accepting capacity (with no donor capacity).³⁵ We do not generally find, in the literature a discussion of PEG being adhesive toward some globular proteins and repulsive toward others. We note, however, the Fraden lab's report of a negative second (cross) virial coefficient between PEG and lysozyme in free solution, based on light scattering.³⁶ This measure of PEG–lysozyme attractions supports our interpretation of Figure 2. Notably, these attractions may cause some penetration of the lysozyme into the PEG layer, but lysozyme penetration through the brush layer to the silica substrate is not indicated or necessary to produce our observations.

A third behavior, the penetration of random PLL coils into PEG–PLL brushes and their subsequent displacement, in Figure 4 is technologically important because it dramatically compromises the protein resistance. Figure 4 demonstrates that an established brush can be completely removed from the surface in less than 5 min, a surprising observation if one expects the PEG corona to osmotically shield the surface from PLL, or if one expects kinetically trapped states at in the adsorbed PLL layer to hinder exchange at the base of the brush.^{11,37,38} Our study demonstrates arrival of PLL to the interface to be the rate limiting step: the adsorbed PLL–PEG brushes are in this sense extremely fragile.

It is worth pointing out that PLL was the only macromolecule tested that was able to penetrate the PEG brushes and proceed with brush displacement. This observation points toward the importance of protein/polypeptide structure in brush interactions. Apparently the dense globular nature of folded proteins is a key component of their exclusion from PEG brushes. The rapid displacement of adsorbed PLL–PEG by PLL suggests a lack of steric repulsions between hydrated PEG tethers and random-coil PLL chains. With PLL able to rapidly penetrate the otherwise protein-repelling brushes, electrostatic attractions to the base of the brush drive PLL adsorption.

The observation of rapid PLL–PEG displacement by PLL further argues that the anchoring PLL sequences are highly

dynamic on the silica substrate. While some studies of polyelectrolyte exchange between solution and an interface reveal sluggish kinetics,^{11,37,38} the PLL anchors of the current study are aided in their removal from the surface by the entropy gain of the PEG tethers when the anchoring sections are released from the substrate. Without these tethers, short PLL train sections might readsorb as rapidly as they desorb, so that the entire PLL chain remains bound despite its dynamic fluctuations: A high density of PEG tethers make local PLL desorption events (involving a few segments) within the trains longer-lasting, facilitating adsorption of homopolymer PLL challengers.

CONCLUSIONS

This study examined the interactions of cationic proteins and polypeptides with cationically anchored PEG brushes whose architectures were previously reported and confirmed here to eliminate adhesion of key serum proteins. The study focused on ionic strength conditions where electrostatic interactions with the negative underlying substrate were screened by the brush.

The work revealed a strong correlation between the sign of the net protein charge and interactions with the brushy surfaces: Negative proteins did not adsorb, while positive proteins/polypeptides were attracted to and retained at the interface. Additional control studies reaffirmed the lack of electrostatic interactions between globular proteins and the underlying substrate, focusing attention on specific interactions between globular proteins and the hydrated PEG tethers. In the case of lysozyme, the greatest adsorption occurred to the brushes having the greatest amount of tethered PEG, a finding running contrary to the literature for general protein repellency of PEG brushes. While the specific mechanism for PEG–lysozyme attractions remains unclear, it is found that cationic lysozyme behaves differently from anionic serum proteins in its interactions with PEG. This finding is contrary to conventional thinking which treats all globular proteins as similar in their interactions with nonionic brushes. These results point to the importance of the interactions between hydrated PEG brushes and globular proteins, which can be highly varied. Apparently there is a sensitivity of this interaction to nature of each protein, a possibility which is generally overlooked in the literature which, based on frequently studied protein models, always assumes domination by steric repulsions between PEG and globular proteins.

Beyond adhesion of the cationic protein lysozyme to the PEG brush corona, the study revealed that cationic random-coil polypeptides, for instance PLL, can rapidly penetrate a hydrated PEG brush, electrostatically interacting with the underlying substrate and displacing the brush. For moderately dense PEG brushes with tethers in the 2000–5000 MW range, such displacement processes are dominated by the arrival rate of PLL to the interface, identical to that for the adsorption of PLL on bare silica. The immediate displacement of the PEG brush demonstrates a potential failure mechanism of these interfaces *in vivo*, and motivates permanent attachment of PEG chains to the substrate.

This work prompts reconsideration of specific PEG–protein interactions, and the nature of the anchoring of PEG groups in the presence of random-coil cationic polyelectrolytes. The findings suggest that, even if the PEG tethers were covalently bound to a substrate, cationic proteins and homopolymers would penetrate and adhere to the brush, or the substrate. Their retention in the brush potentially renders the interface bioadhesive to other proteins and cells, even without displacement of the PEG tethers.

ASSOCIATED CONTENT

S Supporting Information. This material is available free of charge via the Internet at <http://pubs.acs.org>.

ACKNOWLEDGMENT

This work was made possible by support from the National Science Foundation: CBET 0932719, DMR 0805061, DMR 0820506, and the Center for Hierarchical Manufacturing ζ potential facility, under NSF 0531171.

REFERENCES

- (1) Pasche, S.; Voros, J.; Griesser, H. J.; Spencer, N. D.; Textor, M. *J. Phys. Chem. B* **2005**, *109*, 17545.
- (2) Michel, R.; Pasche, S.; Textor, M.; Castner, D. G. *Langmuir* **2005**, *21*, 12327.
- (3) Yang, Z. G.; Zhou, F.; Yuan, J. J.; Ma, L. X.; Zhai, C.; Cheng, S. Y. *Sci. China Ser. B-Chem.* **2006**, *49*, 357.
- (4) Harris, L. G.; Tosatti, S.; Wieland, M.; Textor, M.; Richards, R. G. *Biomaterials* **2004**, *25*, 4135.
- (5) Bergstrand, A.; Rahmani-Monfared, G.; Ostlund, A.; Nyden, M.; Holmberg, K. *J. Biomed. Mater. Res. Part A* **2009**, *88A*, 608.
- (6) Dincer, S.; Turk, M.; Karagoz, A.; Uzunalan, G. *Artif. Cells Blood Substit. Biotechnol.* **2011**, *39*, 143.
- (7) Dalsin, J. L.; Hu, B. H.; Lee, B. P.; Messersmith, P. B. *J. Am. Chem. Soc.* **2003**, *125*, 4253.
- (8) Dalsin, J. L.; Lin, L. J.; Tosatti, S.; Voros, J.; Textor, M.; Messersmith, P. B. *Langmuir* **2005**, *21*, 640.
- (9) Dijt, J. C.; Stuart, M. A. C.; Fleer, G. J. *Macromolecules* **1994**, *27*, 3219.
- (10) Fu, Z. L.; Santore, M. M. *Macromolecules* **1998**, *31*, 7014.
- (11) Sukhishvili, S. A.; Granick, S. *J. Chem. Phys.* **1998**, *109*, 6869.
- (12) Milner, S. T. *Science* **1991**, *251*, 905.
- (13) Pasche, S.; De Paul, S. M.; Voros, J.; Spencer, N. D.; Textor, M. *Langmuir* **2003**, *19*, 9216.
- (14) Huang, N. P.; Michel, R.; Voros, J.; Textor, M.; Hofer, R.; Rossi, A.; Elbert, D. L.; Hubbell, J. A.; Spencer, N. D. *Langmuir* **2001**, *17*, 489.
- (15) Kenausis, G. L.; Voros, J.; Elbert, D. L.; Huang, N. P.; Hofer, R.; Ruiz-Taylor, L.; Textor, M.; Hubbell, J. A.; Spencer, N. D. *J. Phys. Chem. B* **2000**, *104*, 3298.
- (16) Gon, S.; Bendersky, M.; Ross, J. L.; Santore, M. M. *Langmuir* **2010**, *26*, 12147.
- (17) Fu, Z. G.; Santore, M. M. *Colloid Surf. A-Physicochem. Eng. Asp.* **1998**, *135*, 63.
- (18) Kelly, M. S.; Santore, M. M. *Colloid Surf. A-Physicochem. Eng. Asp.* **1995**, *96*, 199.
- (19) Wertz, C. F.; Santore, M. M. *Langmuir* **1999**, *15*, 8884.
- (20) Alexander, S. *J. Phys.* **1977**, *38*, 983.
- (21) de Gennes, P. G. *J. Phys. (Paris)* **1976**, *38*, 1443.
- (22) Gon, S.; Santore, M. M. *Langmuir* **2011**, *27*, 1487.
- (23) Wasilewska, M.; Adamczyk, Z.; Jachimska, B. *Langmuir* **2009**, *25*, 3698.
- (24) Tsapikouni, T. S.; Missirlis, Y. F. *Colloid Surf. B-Biointerfaces* **2007**, *57*, 89.
- (25) Bohme, U.; Scheler, U. *Chem. Phys. Lett.* **2007**, *435*, 342.
- (26) Arai, T.; Norde, W. *Colloids Surf.* **1990**, *51*, 1.
- (27) de Backer, M.; McSweeney, S.; Rasmussen, H. B.; Riise, B. W.; Lindley, P.; Hough, E. J. *Mol. Biol.* **2002**, *318*, 1265.
- (28) Kuehner, D. E.; Engmann, J.; Fergg, F.; Wernick, M.; Blanch, H. W.; Prausnitz, J. M. *J. Phys. Chem. B* **1999**, *103*, 1368.
- (29) Feng, W.; Zhu, S. P.; Ishihara, K.; Brash, J. L. *Langmuir* **2005**, *21*, 5980.
- (30) Zhou, G. Y.; Ma, C. F.; Zhang, G. Z. *Polym. Chem.* **2011**, *2*, 1409.
- (31) Kalasin, S.; Santore, M. M. *Colloid Surf. B-Biointerfaces* **2009**, *73*, 229.

- (32) Deshmukh, V.; Britt, D. W.; Hlady, V. *Colloid Surf. B-Biointer-*
faces **2010**, *81*, 607.
- (33) Adamczyk, Z.; Nattich, M.; Wasilewska, M.; Sadowska, M.
J. Colloid Interface Sci. **2011**, *356*, 454.
- (34) Ortega-Vinuesa, J. L.; Tengvall, P.; Lundstrom, I. *Thin Solid*
Films **1998**, *324*, 257.
- (35) Ostuni, E.; Chapman, R. G.; Holmlin, R. E.; Takayama, S.;
Whitesides, G. M. *Langmuir* **2001**, *17*, 5605.
- (36) Bloustine, J.; Virmani, T.; Thurston, G. M.; Fraden, S. *Phys. Rev.*
Lett. **2006**, *96*.
- (37) Hansupalak, N.; Santore, M. M. *Macromolecules* **2004**, *37*, 1621.
- (38) Santore, M. M. *Curr. Opin. Colloid Interface Sci.* **2005**, *10*, 176.